J. Phys. B: At. Mol. Opt. Phys. **29** (1996) 3235–3244. Printed in the UK

Electron-impact ionization and dissociative ionization of acetylene

S-H Zheng† and Santosh K Srivastava

Jet Propulsion Laboratory, California Institute of Technology, 4800 Oak Grove Drive, Pasadena, CA 91109, USA

Received 29 January 1996

Abstract. A pulsed electron beam and ion extraction system has been employed to measure cross sections for formation of $C_2H_2^+$, C_2H^+, C_2^+, $C_2H_2^{++} + CH^+$, $C_2^{++} + C^+$ and H^+ by electron impact on acetylene (C_2H_2) in the energy range varying from threshold to 800 eV. The relative flow technique has been used to obtain normalized values of cross sections. Appearance potentials (APs) for ionic species are reported. Present values of APs are compared with previously published data.

1. Introduction

Electron-impact ionization studies of acetylene, C_2H_2, have been conducted sporadically for many decades since Tate *et al* (1932, 1935) first investigated the electron-impact properties of C_2H_2. The most recent results are by Davister and Locht (1994, 1995), who studied the dissociative electroionization of C_2H_2, the translational energy distribution and the threshold energies of some channels.

The importance of electron collisional properties of acetylene has been widely recognized for several reasons. C_2H_2 is the simplest molecule among hydrocarbons. It is present in planetary and cometary atmospheres and in the interstellar medium. The distinctive features of C_2H_2 in the vacuum ultraviolet (VUV) spectrum were first detected in the atmospheres of Saturn by the International Ultraviolet Explorer (IUE) satellite (Moos and Clarke 1979), and later in the atmosphere of Titan (Smith *et al* 1982), Uranus (Encrenaz *et al* 1986, Herbert *et al* 1987) and Jupiter (Owen *et al* 1987). The concentration of C_2H_2 in the atmosphere of Earth is expected to nearly double by the year 2030 due to the increased use of automobiles (Varanasi *et al* 1983). Its detection by mass spectrometric methods, which employ electron-impact ionization, provides a very sensitive method of monitoring its presence. Fusion plasma devices often use graphite as material for their inner walls in order to reduce radiation losses. Hydrocarbon products are produced at these walls. The region close to these walls (plasma edge) plays an important role in the characteristics of the cold plasma edge as well as the hot plasma interior (Tawara and Phaneuf 1988, Tawara *et al* 1992). It is also used in the semiconductor industry for the deposition of diamond film (McMaster *et al* 1995). Electron collision properties are important for modelling the plasma containing C_2H_2.

Cross sections for the formation of various ionic fragments due to electron impact on C_2H_2 have been measured only by Gaudin and Hagemann (1967) in the electron-impact

† NRC-NASA Resident Research Associate.

0953-4075/96/143235+10$19.50

energy range of 100 to 2000 eV. For most low-temperature plasma modelling purposes values of cross sections below 100 eV electron-impact energy, especially near the threshold of formation of ions, are needed. The absence of these cross sections prompted us to undertake the present work.

In this paper we present our values of cross sections for the formation of $C_2H_2^+$, C_2H^+, C_2^+, $C_2H_2^{++} + CH^+$, $C_2^{++} + C^+$ and H^+ by electron impact on C_2H_2 in the energy range from threshold to 800 eV. We also measured appearance potentials (APs) of ionic species observed in our experiment.

2. Experimental arrangement and method

2.1. Experimental arrangement

The experimental set-up used in this work has been described in detail in previous publications from our group (e.g. Krishnakumar and Srivastava 1988, Rao and Srivastava 1993). A schematic diagram of the apparatus used in the present measurements is shown in figure 1.

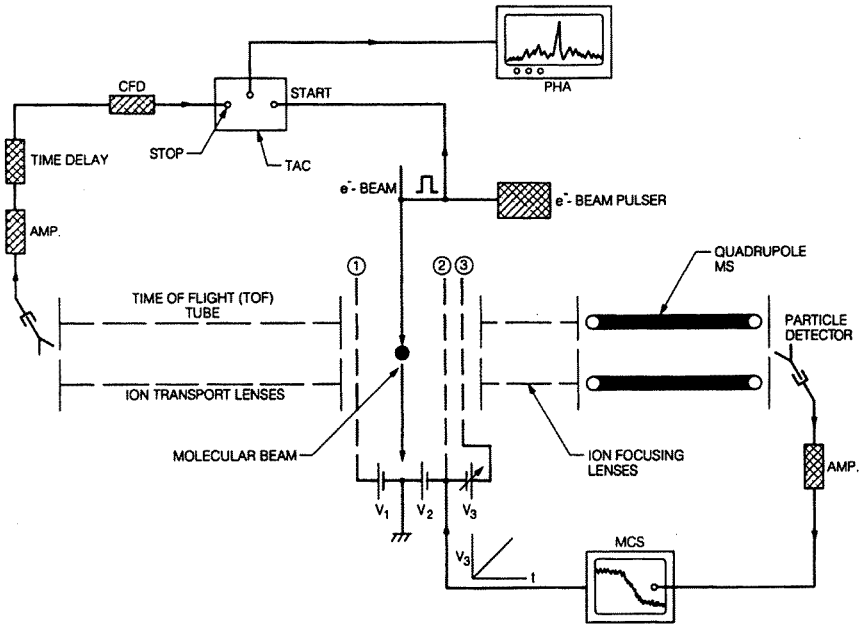

Figure 1. Schematic diagram of the experimental set-up.

Our system consists of five major parts: a magnetically collimated (≅100 G) pulsed electron gun, a capillary array to inject target gas, a pulsed ion extraction system, a quadrupole (QMS) or a time-of-flight mass spectrometer (TOFMS), and electronic devices for data acquisition and analysis. The first four are enclosed in a vacuum chamber which is pumped by a turbo-molecular pump.

The base pressure of the chamber without injection of target gases typically remains below 3×10^{-8} torr and rises to about 8×10^{-8} torr when they are flowed into the chamber. The pulsed electron beam is obtained by applying to the filament a square electrical pulse with rise time of the order of 10 ns or less, duration of about 200 ns and height of 10 V.

We usually set the pulse frequency to 30 kHz, which can produce an average current of 5 nA as measured by a simple Faraday cup. It is estimated that the energy resolution of the electron beam is, in general, about 0.5 eV at full width at half maximum (FWHM).

Ions are produced after the pulsed electron beam impacts the target gas. Since the electron pulse width is about 200 ns or less the energetic ions do not travel too far from the ionization region. Right after the electron pulse, a pulsed electric field ($\cong$ 100 V cm^{-1}) is imposed on the collision region to extract all ions and focus them at the entrance of the QMS or the TOFMS. Details of the ion extraction method employed by us can be found in one of our previous publications (Rao and Srivastava 1993). Subsequently, the ions are mass selected and detected by a charged particle detector (channeltron), which converts the detected ion into an electric pulse. This pulse is subsequently amplified by a fast amplifier which changes it into a TTL pulse. The MCS records the number of TTL pulses as a function of electron impact energy.

2.2. The method of normalization and error estimation

With the experimental set-up described above, the relative intensities for each ionic species as a function of electron-impact energy are obtained. A plot of intensity of a particular ionic species as a function of electron-impact energy is generally called an 'ionization efficiency curve'.

Since the ion intensity is directly proportional to the value of cross section, this curve also represents the dependence of the cross section on the electron-impact energy. In our experimental procedure the electron energy is continuously varied from 0 to 800 eV in such a way that the electron beam current, as measured by the Faraday cup, remains constant. It is hoped that this constancy in current ensures that all other collision conditions remain the same except for the electron beam energy. However, in practice the overlap volume (i.e. the volume enclosed by the intersection of electron beam, molecular beam and view cone of the mass analyser) changes slightly. An estimate of this change can be made by using a target for which the ionization efficiency curve is accurately known. For rare gases they are known with an accuracy of about $\pm$5% (Krishnakumar and Srivastava 1988 and references therein). For the present experiment we used the curve for Ne for obtaining correction factors for the overlap as a function of electron-impact energy. These factors were employed for obtaining the correct shapes of all 'ionization efficiency curves'.

In order to obtain values of cross sections, the 'ionization efficiency curves' need a method of normalization. For this purpose we utilized the relative flow technique (Srivastava *et al* 1975). This technique is well established now and has been shown to generate accurate values of cross sections. Detailed description of the normalization procedure can be found in Rao and Srivastava (1993). Briefly, the method utilizes a gas for which cross section values are accurately known. A beam of this gas is formed by flowing it through the capillary array under the conditions of molecular flow. The ion signal is then recorded at a fixed electron impact energy (e.g. 100 eV). The flow of this gas is then stopped and replaced by the gas under study (C_2H_2) and the flow rate is adjusted so that, again, it is in the molecular flow regime. Other experimental conditions are kept unchanged. The ion signal of the gas under study is then recorded.

The ion intensities and cross sections for two gases 'u' (stands for unknown) and 's' (stands for standard) are related through the following relation:

$$\frac{\sigma_u(E)}{\sigma_s(E)} = \frac{I_u(E)}{I_s(E)} \left(\frac{m_u}{m_s}\right)^{1/2} \frac{F_u}{F_s} \frac{K(m_u)}{K(m_s)} \tag{1}$$

where E is the energy of the electron beam, $\sigma_u(E)$ and $\sigma_s(E)$ the ionization cross sections of the species under study and species for which cross sections are accurately known, respectively, m_u and m_s are the respective mass ratios, $I_u(E)$ and $I_s(E)$ their respective ion intensities, $F_u(E)$ and $F_s(E)$ their respective gas flow rates, and $K(m_u)$ and $K(m_s)$ are factors which determine the transmission and detection efficiency of the experimental apparatus for the two species. The $K(m_u)$ and $K(m_s)$ factors can be measured by applying the above formula and utilizing the electron ionization cross sections of H_2, N_2 and Ne, together with the procedure described by Krishnakumar and Srivastava (1988).

It is estimated that the present results are accurate to within $\pm 13\%$. The basis for this estimation is described by Krishnakumar and Srivastava (1988).

3. Method for measuring APs

In order to determine the energy at which ions begin to appear as the electron impact energy is increased from 0 to higher values we first record the 'ionization efficiency curve' for each ionic species over a short interval ($\cong$ 40 eV) of impact energy near the threshold of its production. A typical 'ionization efficiency curve' near the threshold region is shown in figure 2. The APs from such curves are obtained by applying the following two methods.

(i) Linear extrapolation approach. A straight line is drawn through the linear portion of the ionization efficiency curve near the threshold. This line is extrapolated to intersect the x-axis (electron energy axis). The value of energy at the intersection is the value of AP (Rosenstock *et al* 1977). However, in general the energy of the electron beam is not the same as the energy read by a voltmeter employed for measuring the voltage between the filament and the ground due to various factors, especially the contact potentials. Therefore, an ionization efficiency curve for a gas such as Ne or Ar is obtained first and a correction factor is determined. This correction factor is applied to the ionization efficiency curve of the species under study.

(ii) Lift-off approach. In this method the position where the ionization efficiency curve begins to rise above the constant background is recorded. Again, as done in the previous method, the energy scale is calibrated by employing the AP of a rare gas atom.

We estimate that, in spite of the fact that our energy resolution is only 0.5 eV, APs determined by using the above two methods are accurate to within 0.25 eV.

4. Results and discussion

Figure 3 shows a mass spectrum of C_2H_2 generated by 100 eV electron impact. As mentioned in the previous section, two types of mass analysers were employed in the present study: a quadrupole mass spectrometer (QMS) and a time-of-flight mass spectrometer (TOFMS). Both of them provided consistent results. Our QMS was not capable of distinguishing the H^+ signal from the background at zero-mass position in the spectra. However, measurement of the H^+ signal could easily be obtained by the TOFMS.

Two types of measurements were performed by us. One was concerned with the values of cross sections and the other was dedicated to the measurement of values of appearance potentials (APs) of various fragment ions. In the following the results of these two measurements will be presented.

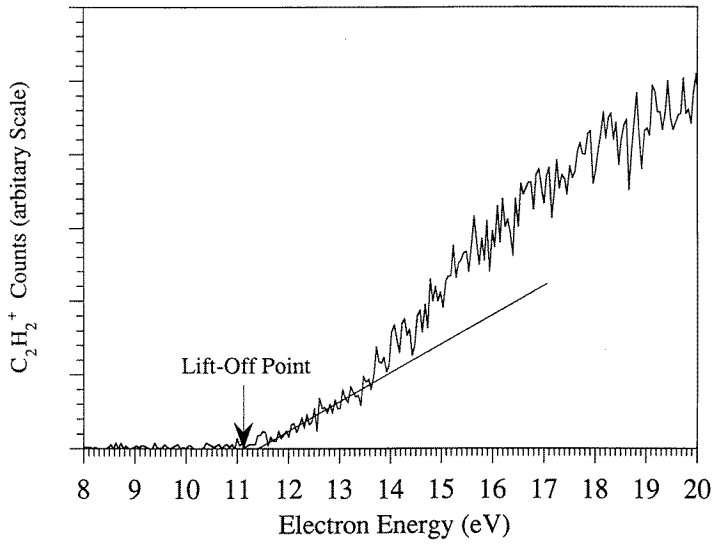

Figure 2. A typical 'ionization efficiency curve' near the threshold region of ion production ($C_2H_2^+$ in the present case).

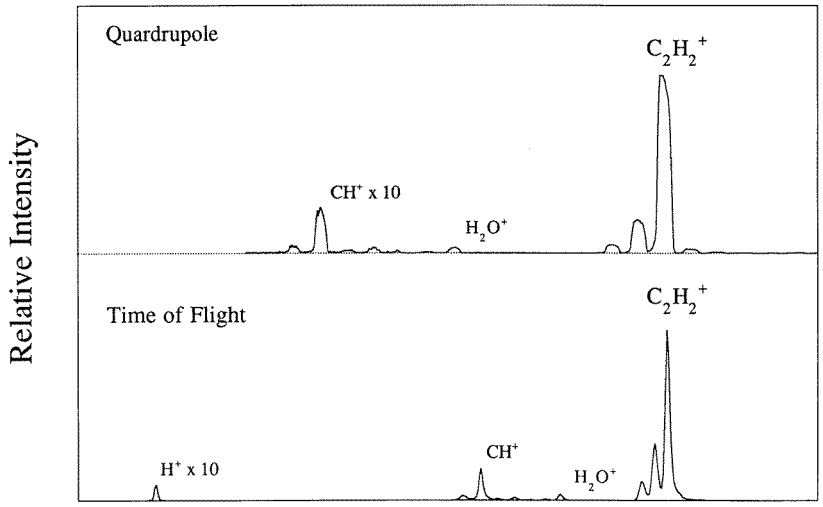

Figure 3. QMS and TOFMS spectra of C_2H_2 at 100 eV electron impact energy.

4.1. Measurement of cross sections

As a result of electron impact the following ions were detected: $C_2H_2^+$, C_2H^+, C_2^+, $C_2H_2^{++} + CH^+$, $C_2^{++} + C^+$ and H^+. Since $C_2H_2^{++}$ cannot be distinguished from CH^+ and, similarly, C_2^{++} cannot be differentiated from C^+ in our experimental arrangement we measured combined cross sections for them. Cross sections for all species mentioned above are presented in table 1. Total ionization cross sections are also presented in this table which were obtained by summing individual cross sections. It was assumed that contributions made by ionization processes other than those observed in the present experiment had negligible effects on the total ionization cross sections presented here.

Table 1. Ionization cross sections for the production of various ionic species by electron impact on C_2H_2 in units of 10^{-18} cm^2. Estimated accuracy of these cross sections is within ±13%.

Energy (eV)	$C_2H_2^+$	C_2H^+	C_2^+	CH^+	C^+	H^+	Total ionization
20	158.9	6.07					165.0
25	248.2	39.5	1.54	0.799		2.92	293.0
30	287.0	56.0	10.1	3.43	1.03	8.02	365.6
35	304.0	62.1	14.8	5.56	2.29	14.6	403.3
40	314.3	66.8	18.0	8.64	4.00	21.9	433.6
45	320.1	69.3	19.1	12.4	4.73	27.8	453.4
50	325.2	70.4	19.6	15.2	5.21	32.8	468.5
55	329.0	70.9	19.9	18.4	5.57	36.5	480.3
60	333.9	71.2	20.1	20.7	5.78	38.9	490.6
65	336.2	71.5	20.3	22.5	5.98	40.7	497.3
70	339.0	71.7	20.5	24.6	6.10	41.6	503.5
75	340.3	71.7	20.6	26.0	6.23	42.1	506.8
80	342.4	71.6	20.5	26.7	6.33	42.3	509.9
85	343.8	71.4	20.5	27.3	6.42	42.5	512.0
90	343.6	71.3	20.4	27.8	6.51	42.5	512.1
95	343.5	71.1	20.3	28.2	6.54	42.5	512.1
100	341.6	71.0	20.2	28.4	6.62	42.2	510.0
105	337.9	70.7	20.0	28.5	6.66	41.8	505.6
110	335.0	70.6	19.9	28.5	6.72	41.1	501.9
115	332.9	70.4	19.7	28.5	6.75	40.4	498.6
120	330.1	70.3	19.5	28.4	6.77	39.6	494.6
125	327.0	70.0	19.3	28.1	6.78	39.0	490.2
130	324.3	69.6	19.0	27.9	6.78	38.4	486.1
135	321.6	69.2	18.7	27.5	6.77	37.8	481.5
140	318.7	68.4	18.4	27.1	6.73	37.1	476.5
145	314.2	67.8	18.2	26.8	6.69	36.5	470.2
150	310.1	66.9	17.9	26.4	6.64	35.8	463.8
155	306.0	66.2	17.7	26.0	6.55	35.2	457.6
160	302.1	65.6	17.4	25.7	6.48	34.5	451.7
165	298.4	64.8	17.2	25.2	6.42	33.9	445.8
170	295.6	63.9	17.1	24.9	6.37	33.2	441.0
175	292.8	63.1	16.9	24.6	6.30	32.5	436.2
180	289.5	62.4	16.7	24.2	6.22	31.8	430.8
185	286.1	61.8	16.5	24.0	6.16	31.2	425.7
190	283.2	61.2	16.3	23.8	6.10	30.6	421.2
195	280.2	60.5	16.1	23.5	6.04	29.8	416.3
200	277.7	60.0	15.9	23.3	5.98	29.2	412.1
225	263.2	56.9	15.1	21.9	5.67	26.3	389.0
250	250.3	54.1	14.1	20.5	5.39	23.8	368.3
275	236.8	51.2	13.3	19.3	5.09	21.9	347.5
300	225.0	48.9	12.4	18.1	4.78	20.4	329.6
350	204.5	44.8	11.0	15.9	4.18	18.0	298.3
400	187.1	41.2	9.83	14.1	3.70	15.8	271.7
450	173.8	38.0	8.75	12.4	3.32	14.3	250.6
500	161.3	35.4	7.93	11.3	3.00	12.8	231.6
550	149.7	33.2	7.27	10.1	2.75	11.2	214.2
600	140.4	31.3	6.76	9.36	2.55	10.2	200.6
650	131.3	29.3	6.22	8.54	2.38	9.72	187.5
700	122.0	27.2	5.69	7.75	2.24	9.18	174.1
750	115.9	25.9	5.31	7.18	2.15	8.51	164.9
800	108.7	24.3	4.89	6.56	2.04	8.02	154.4

As mentioned before, the only data which provide values of cross sections are by Gaudin and Hagemann (1967). Tate and Smith (1932) also measured the efficiency for the production of all ions, which can be converted to obtain the total ionization cross section. In a later paper they published relative values of intensities for the formation of various fragment ions (Tate *et al* 1935) resulting from the dissociation of C_2H_2. From these two publications and with the assumption that the transmission and detection efficiencies for all the reported ionic species were equal, we can obtain ionization cross sections for all ionic products recorded by Tate *et al* (1935).

Our results for the formation of $C_2H_2^+$, C_2H^+ and C_2^+ agree very well with the data of Gaudin and Hagemann within the combined errors of two measurements and with the normalized values of Tate *et al*. The cross sections of them as a function of electron impact energy are shown in figure 4.

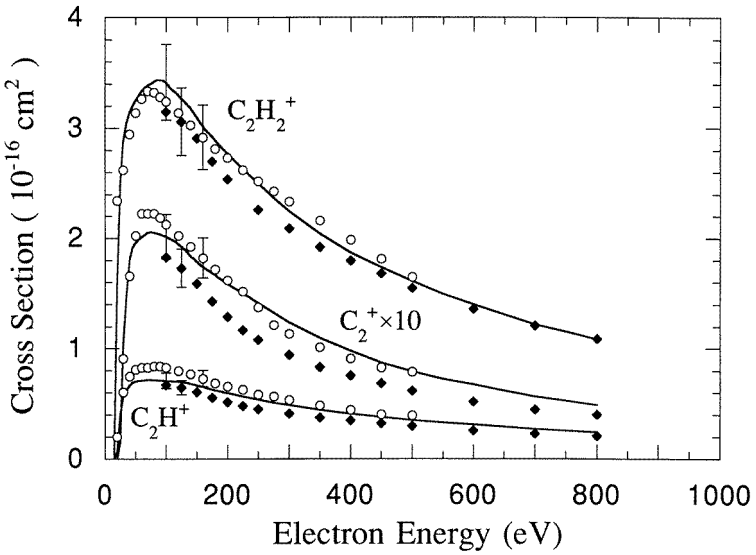

Figure 4. Ionization cross sections as a function of electron-impact energy for the processes $e+C_2H_2 \rightarrow C_2H_2^+$, $e+C_2H_2 \rightarrow C_2H^+$ and $e+C_2H_2 \rightarrow C_2^+$. Full curve: present measurements, (○) Tate *et al* (1935), (♦) Gaudin and Hagemann (1967). For the process $e + C_2H_2 \rightarrow C_2^+$, the data of all measurements are multiplied by a factor of 10.

However, the agreement between the present results and previous ones is not good for $C_2H_2^{++} + CH^+$, $C_2^{++} + C^+$ and H^+. As can be seen from figure 5 the differences are large. The only explanation for the large differences that can be offered is that previous experiments, probably, did not collect ions completely from the ionization region due to the fact that these ions might have possessed a considerable amount of kinetic energy when they were born. We employed a pulsed ion extraction technique which ensured a complete collection of all energetic ions. Thus, the signal collected by us is higher than those reported previously for fragment ions.

Figure 6 shows our results for total ionization cross sections as a function of electron-impact energy. They agree very well with that of Tate *et al*'s measurement. However, our total cross section values are generally 23% higher than that of Gaudin and Hagemann's measurements.

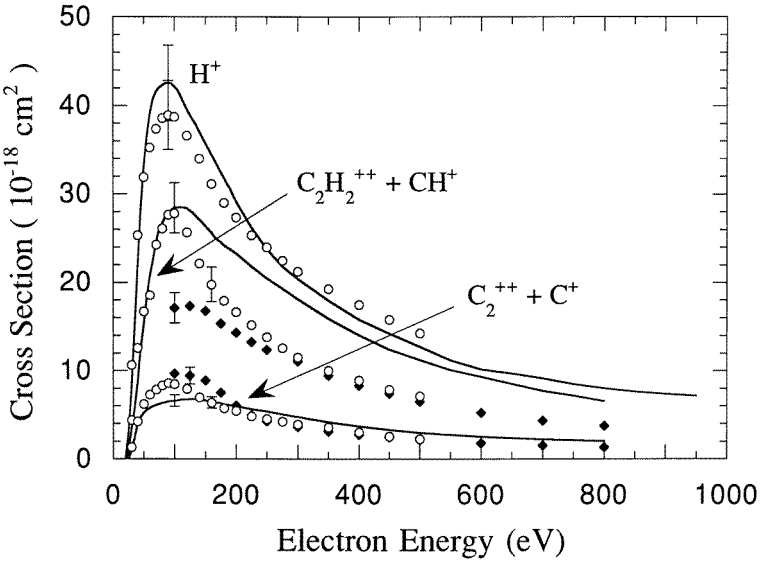

Figure 5. Ionization cross sections as a function of electron-impact energy for the processes $e + C_2H_2 \rightarrow H^+$, $e + C_2H_2 \rightarrow C_2H_2^{++} + CH^+$ and $e + C_2H_2 \rightarrow C_2^{++} + C^+$. Full curve; present measurement, (○) Tate *et al* (1935) multiplied by 1.5, (♦) Gaudin and Hagemann (1967) multiplied by 2.

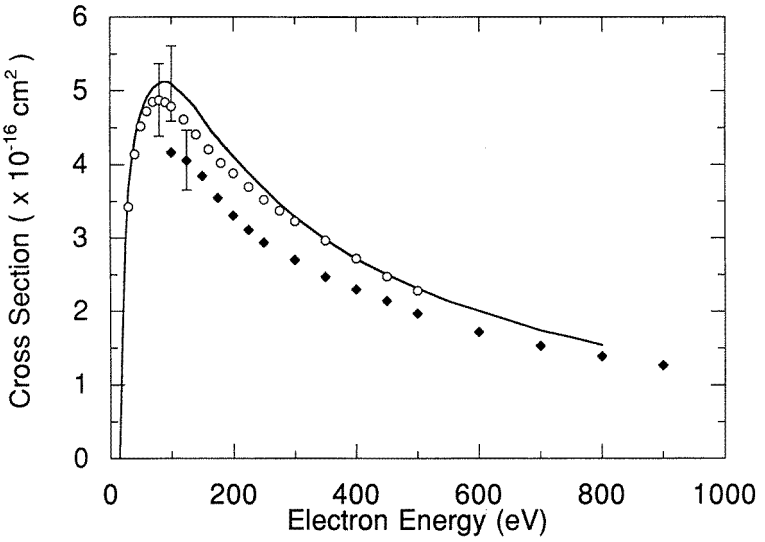

Figure 6. Total ionization cross section as a function of electron impact energy. Full curve: present measurements, (○) Tate *et al* (1932), (♦) Gaudin and Hagemann (1967).

4.2. Measurement of APs

Present data on APs, listed in table 2, are compared with the two most recent measurements. Data reported prior to 1986 are designated as 'other work' and references for them can be found in Plessis and Marmet (1986). The data designated as 'calculation' are determined

by the thermochemical method using the dissociation and ionization energies published previously (Rosenstock 1977, Davister and Locht 1994, 1995). The possible dissociative channels are suggested in table 2. It is satisfying to note that the present data agree well with those obtained previously.

Table 2. Measured and calculated APs in eV.

Species	Possible channel	Calculation	This work	Davister and Locht (1994)	Plessis and Marmet (1986)	Other work[a]
$C_2H_2^+$			11.4 ± 0.2		11.41 ± 0.01	11.401 ± 0.007
C_2H^+	$C_2H^+ + H$	17.0	17.2 ± 0.2	$17.30 + 0.11$ 18.27 ± 0.10	16.70 ± 0.10	16.4 ± 0.8 to 17.45 ± 0.1
C_2^+	$C_2^+ + 2H$	22.33	22.9 ± 0.3		22.60 ± 0.12	22.7 ± 0.1 to 23.8 ± 0.3
CH^+	$CH^+ + C + H$	23.94	23.6 ± 0.5		23.9 ± 0.2	24.1 ± 0.1 and 24.02 ± 0.03
C^+	$C^+ + H + CH$	24.559	24.9 ± 0.5			24.5 ± 1.0
H^+	$H^+ + C_2H$	18.93	19.2 ± 0.5	18.93 ± 0.2		

[a] Data published prior to Plessis and Marmet where further references are cited.

5. Conclusion

Our results show that the pioneering work of Tate *et al* (1932, 1935) is quite reliable and agrees well with our total ionization cross section values. However, for fragment ions of $C_2H_2^{++} + CH^+$, $C_2^{++} + C^+$ and H^+ the differences are large and indicate that they did not collect all of the ion signal from the collision region due to high kinetic energies which the fragment ions may possess. This calls for measurement of kinetic energies of these fragment ions in the future.

Our results on appearance potentials (AP) for all ionic fragments observed in this experiment have been compared with the previous measurements and thermochemical results. We find that our results agree very well with them within the experimental errors. This has allowed us to support the possible channels of dissociation which are important for understanding the chemistry of the plasma where C_2H_2 is present.

Acknowledgments

The research presented in this publication was carried out at the Jet Propulsion Laboratory and was sponsored by the National Aeronautics and Space Administration. One of us (SZ) would like to thank NRC, Washington, DC, for a Resident Research Associate grant during the course of this work.

References

Davister M and Locht R 1994 *Chem. Phys.* **189** 805
——1995 *Chem. Phys.* **191** 333
Encrenaz T, Combes M, Atreya S K, Romani P N, Moore V, Hunt G, Wagener R and Caldwell J 1986 *Astron. Astrophys.* **162** 317
Gaudin A and Hagemann R 1967 *J. Chem. Phys.* **64** 1209
Herbert F, Sandel B R, Yelle R V, Holberg J B, Broadfoot A L, Shemansky D E, Atreya S K and Romani P N 1987 *J. Geophys. Res.* **92** 15 093

Krishnakumar E and Srivastava S K 1988 *J. Phys. B: At. Mol. Opt. Phys.* **21** 1055
McMaster M C, Hsu W L, Coltrin M E, Dandy D S and Fox C 1995 *Diamond Rel. Mater.* **4** 1000
Moos H W and Clarke J T 1979 *Astrophys. J.* **229** L107
Owen T C, Caldwel J, Rivolo A R, Moore V, Lane A L, Sagan C, Hunt H and Ponnamperuma C 1987 *Astrophys. J.* **236** L39
Plessis P and Marmet P 1986 *Int. J. Mass Spectrosc. Ion Proc.* **70** 23
Rao M V V S and Srivastava S K 1993 *J. Geophys. Res.* **98** 13 137
Rosenstock H M, Draxl K, Steiner B W and Herron J T 1977 *J. Phys. Chem., Ref. Data* **6**
Smith P T, Yoshino K, Parkinson W H, Ito K and Stark G 1991 *J. Geophys. Res.* **96** 17 529
Srivastava S K, Chutjian A and Trajmar S 1975 *J. Phys. Chem.* **63** 2659
Tate J T and Smith P T 1932 *Phys. Rev.* **39** 270
Tate J T, Smith P T and Vaughan A L 1935 *Phys. Rev.* **48** 525
Tawara H and Phaneuf R A 1988 *Comment. At. Mol. Phys.* **22** 963
Tawara H, Tonuma T, Kumagai H and Matsuo T 1992 *J. Phys. B: At. Mol. Opt. Phys.* **25** L423
Varanasi P, Giver L P and Valero F P J 1983 *Quant. Spectrosc. Radiat. Transfer* **30** 497